Regular Article

Turkish Plants, Including Quercetin and Oenothein B, Inhibit the HIV-1 Release and Accelerate Cell Apoptosis

Yurika Tahara,[a] Mikako Fujita,[a] Tianli Zhang,[b] Dongxing Wang,[c] Hiroshi Tateishi,[a] Akihiro Togami,[a] Perpetual Nyame,[b] Hiromi Terasawa,[b] Nami Monde,[b] Joyce Appiah-Kubi,[b] Wright Ofotsu Amesimeku,[b] Doaa Husham Majeed Alsaadi,[c] Mikiyo Wada,[d] Koji Sugimura,[c] Sevgi Gezici,[e] Halilibrahim Ciftci,[a,f] Faruk Karahan,[g] Nazim Sekeroglu,[e] Masami Otsuka,[a,f] Tomohiro Sawa,[b] Yosuke Maeda,[b] Takashi Watanabe,*[,c] and Kazuaki Monde*[,b]

[a] *Medicinal and Biological Chemistry Science Farm Joint Research Laboratory, Faculty of Life Sciences, Kumamoto University, Kumamoto 862–0973, Japan:* [b] *Department of Microbiology, Faculty of Life Sciences, Kumamoto University, Kumamoto 860–8556, Japan:* [c] *Department of Medicinal Plant, Faculty of Life Sciences, Kumamoto University, Kumamoto 862–0973, Japan:* [d] *Department of Instrumental Analysis, Faculty of Life Sciences, Kumamoto University, Kumamoto 862–0973, Japan:* [e] *Department of Medical Sciences, Faculty of Medicine, Gaziantep University, Gaziantep 27300, Turkey:* [f] *Science Farm Ltd., Kumamoto 862–0976, Japan: and* [g] *Department of Biology, Faculty of Science and Literature, Hatay Mustafa Kemal University, Hatay 31060, Turkey.*

Received May 16, 2023; accepted August 31, 2023

The introduction of combined anti-retroviral therapy (cART) in 1996, along with a continual breakthrough in anti-human immunodeficiency virus-1 (HIV-1) drugs, has improved the life expectancies of HIV-1-infected individuals. However, the incidence of drug-resistant viruses between individuals undergoing cART and treatment-naïve individuals is a common challenge. Therefore, there is a requirement to explore potential drug targets by considering various stages of the viral life cycle. For instance, the late stage, or viral release stage, remains uninvestigated extensively in antiviral drug discovery. In this study, we prepared a natural plant library and selected candidate plant extracts that inhibited HIV-1 release based on our laboratory-established screening system. The plant extracts from *Epilobium hirsutum* L. and *Chamerion angustifolium* (L.) Holub, belonging to the family Onagraceae, decreased HIV-1 release and accelerated the apoptosis in HIV-1-infected T cells but not uninfected T cells. A flavonol glycoside quercetin with oenothein B in Onagraceae reduced HIV-1 release in HIV-1-infected T cells. Moreover, extracts from *Chamerion angustifolium* (L.) Holub and *Senna alexandrina* Mill. inhibited the infectivity of progeny viruses. Together, these results suggest that *C. angustifolium* (L.) Holub contains quercetin with oenothein B that synergistically blocks viral replication and kills infected cells *via* an apoptotic pathway. Consequently, the plant extracts from the plant library of Turkey might be suitable candidates for developing novel anti-retroviral drugs that target the late phase of the HIV-1 life cycle.

Key words human immunodeficiency virus-1 (HIV-1), quercetin, oenothein B, Onagraceae, flavonol, apoptosis

INTRODUCTION

For approximately four decades since the discovery of human immunodeficiency virus-1 (HIV-1) as the causative agent of AIDS, efforts to curb the AIDS pandemic have been overwhelming.[1)] Aside from public awareness, antiretroviral therapeutic agents represented massive milestones.[2)] An enormous number of Food and Drug Administration (FDA)-approved antiretrovirals, with the hallmark of attaining low viremia by inhibiting unique processes in HIV-1 replication, are clinically available worldwide. A more recognizable measure to mitigate the persisting challenges in combined antiretroviral therapy (cART) is the urgency to develop a drug with a new inhibitory mechanism that targets multiple stages of the HIV-1 life cycle. With regard to antiretroviral therapy, the late stages of the viral life cycle remain unexplored for potential drug targets.[3)]

During the late stage of the HIV-1 replication cycle, the HIV-1 precursor Gag (Pr55) is synthesized and forms a viral particle at the plasma membrane (PM).[4,5)] HIV-1 Gag comprises four major domains and two small spacer regions: matrix (MA), capsid (CA), nucleocapsid (NC), late domain (p6), and spacer peptides (SP1 and SP2).[6)] Myristoylation and the highly basic region in MA (p17) are critical for membrane targeting and binding at the PM.[7–10)] The MA domain coordinates the incorporation of enveloped glycoprotein (Env) into immature virions through the interactions between MA and Env at the PM.[11,12)] Not only does CA (p24) participate in the formation of an immature Gag lattice through Gag multimerization[13,14)] but also in the formation of a cone-shaped core following HIV-1 protease cleavage of immature virions.[15)] NC (p7) is also associated with Gag multimerization and packaging of viral genomic RNA into virions.[16)] In addition to hijacking the cellular endosomal sorting complex required for transport machinery to attain viral pinch-off, p6 assembles the viral accessory gene (Vpr) into virions.[17,18)] These remarkable roles of Pr55 during HIV-1 assembly make it a promising drug target.

Certain botanical molecules isolated from natural sources have been identified as anti-HIV-1 agents.[19–21)] Lectin (Griffithsin), isolated from the red alga *Griffithsia* sp., inhibits HIV-1 entry by interfering with the viral enveloped glycoprotein.[22,23)] Coumarins isolated from *Clausena lenis* regulate HIV-1 post-

* To whom correspondence should be addressed. e-mail: wtakashi@kumamoto-u.ac.jp; monde@kumamoto-u.ac.jp

© 2023 The Pharmaceutical Society of Japan

entry by inhibiting reverse transcriptase activities.[24] Terpenes were isolated from *Daphne genkwa* Siebold & Zucc. and were found to impede HIV-1 replication in the early stages of the viral life cycle.[25] The synthetic derivative (bevirimat) of betulinic acid isolated from *Syzygium claviflorum* is a drug candidate as an HIV-1 maturation inhibitor.[26–28] However, the FDA has not authorized the clinical use of bevirimat.[29,30] Several drug discovery studies aimed at obstructing the functions of HIV-1 Gag have focused only on small synthetic molecules that are not from the natural components.

The relevance of natural compounds in treating HIV-1 needs to be better understood. In this study, we focused on discovering natural compounds that target HIV-1 Gag and suppress HIV-1 replication in the late phase of the HIV-1 life cycle. We have discussed the mechanism through which the plant extracts induce apoptosis in HIV-1-infected T cells. The findings of this study indicate that the flavonols in the Onagraceae family might be suitable candidates that target the late phase of the HIV-1 life cycle.

MATERIALS AND METHODS

Turkish Plants The collection of plant materials and extraction methods used in this study have been described previously.[31] Plant materials were collected from the roots, stems, twigs, leaves, fruits, shells, and seeds. The plants were identified by F.K. These were cleaned and dried at 50 °C for 7 to 10 d using a DRG400AA (ADVANTEC, Tokyo, Japan). Subsequently, the dried material was soaked in 70% ethanol. Ethanol was evaporated, and the samples were redissolved in dimethyl sulfoxide (DMSO) (10 mg/mL) to prepare a Turkish plant library comprising 164 samples. The plant materials are stored in the Faculty of Life Sciences, Kumamoto University.

Plasmids HIV-1 molecular clone pNL4-3/KFS contains a frameshift mutation that disrupts Env expression.[32] pNL4-3/GagVenus, which encodes Gag fused to the mVenus variant of yellow fluorescent protein (YFP) fusion at the C-terminus of Gag, has been described in previous studies.[8] The Vpr protein was tagged with an 11 amino acid peptide tag (HiBiT) using PCR amplification. The sequence of the first and second forward primers was GTATCGGATCCATGGAACAAGCCCCAGAAGACCAA, which encoded the Vpr and restriction site (*Bam*HI). The sequence of the first reverse primer was CGGCTGGCGGCTGTTCAAGAA GATTAGCTAGGTCGACCAGCTGTG, which encoded the HiBiT tag and restriction site (*Sal*I). The sequence of the second reverse primer was GAAATGGAGCCAGTAGATCCG TGAGCGGCTGGCGGCTGTTCAAGA, which encoded the HiBiT tag and HIV-1 Vpr. The PCR product (Vpr-HiBiT) was inserted into pRDI292 using restriction enzymes *Bam*HI and *Sal*I. The U3 region was inserted into the 5′-untranslated region of pRDI292 to reconstruct the intact 5′-long terminal repeat (LTR). Thus, pRDI292/Vpr-HiBiT encoded LTR-driven Vpr-HiBiT and SV40-driven puromycin resistance genes. Furthermore, to avoid packaging the pRD292/Vpr-HiBiT genes into HIV-1 virions, the packaging signal was removed from the pRDI292/Vpr-HiBiT construct.

Cells 293T cells were cultured in Dulbecco's modified Eagle's medium (Sigma-Aldrich, St. Louis, MO, U.S.A.) supplemented with 10% fetal bovine serum (FBS). Jurkat/Vpr-HiBiT, CEM-GFP and MT-2 cells were cultured in RPMI1640 medium (Thermo Fisher Scientific, Waltham, MA, U.S.A.) with 10% FBS. CEM-GFP cells were obtained through the AIDS Research and Reference Reagent Program, Division of AIDS, NIAID, NIH, from Dr. Jacques Corbeil.[33]

Generation of Jurkat/Vpr-HiBiT Cell Lines pRDI292/Vpr-HiBiT was digested and linearized using the *Hpa*I restriction enzyme. According to the manufacturer's instructions, the linearized plasmid was transfected into Jurkat T cells using AMAXA Nucleofector (Lonza, Basel, Switzerland). As described above, pRDI292/Vpr-HiBiT transduction using a lentiviral vector was unavailable due to the deletion of the packaging signal. Transfected cells were cultured in RPMI1640 with puromycin for approximately 30 d. Next, cells that permanently expressed the puromycin resistance gene were selected.

Measurement of Nanoluciferase Luminescence Jurkat/Vpr-HiBiT cells were infected with VSV-G-pseudotyped NL4-3/KFS cells. At 15 h post-infection, the infected cells were cultured in RPMI1640 with the plant extracts, myricetin, and quercetin for 2 d. The supernatant was harvested from the infected Jurkat/Vpr-HiBiT cells, and luminescence was measured using the Nano-Glo® HiBiT Lytic Detection System (Promega, Madison, WI, U.S.A.), according to the manufacturer's instructions. Briefly, the cell supernatant was mixed with Nano-Glo® HiBiT Lytic Buffer (Promega), LgBiT, and substrate. Luciferase activity was measured using a GloMax® Discover System (GM3000) (Promega).

p24 Gag Enzyme-Linked Immunosorbent Assay (ELISA) The supernatant was harvested from the infected Jurkat/Vpr-HiBiT cells. Gag proteins in the supernatant were quantified using a p24 ELISA (ZeptoMetrix, NY, U.S.A.), according to the manufacturer's instructions.

Confocal Microscopy 293T cells were co-transfected with pHCMV-G (VSV-G), pCMVNLGagPolRRE,[34] and pNL4-3/GagVenus. The virus was harvested for 2 d post-transfection. In contrast, Jurkat/Vpr-HiBiT cells were infected with VSV-G-pseudotyped NL4-3/GagVenus cells. At 15 h post-infection, the infected cells were cultured with the plant extracts for 1 d and then fixed with 4% paraformaldehyde (PFA) (Wako, Osaka, Japan) for 30 min at 4 °C. The cells were washed once with phosphate-buffered saline, mixed with Fluoromount-G (Dako, Glostrup, Denmark), and then plated on a microscope slide (Matsunami, Osaka, Japan). Images of 35–50 fields were recorded using a Zeiss LSM 700 laser scanning confocal microscope (Carl Zeiss, Oberkochen, Germany). At least 25 cells expressing GagVenus were examined for each condition and counted using the ImageJ software program version 10.2 (NIH). The top images of the cell membrane were analyzed for the counting of Gag punctate. A threshold was set in ImageJ to select GagVenus positive pixels greater than 10 relative fluorescence units (on a 100 to 255, 8-bit scale) above the calculated background. The GagVenus positive pixels per cell were then counted using analyze particles in ImageJ.

3-(4,5-Dimethylthiazol-2-yl)-2,5 Diphenyl Tetrazolium Bromide (MTT) Assay Jurkat/Vpr-HiBiT cells were cultured with plant extracts, myricetin, and quercetin (Tokyo Chemical Industry Co., Ltd., Tokyo, Japan) for 2 d. The cells were then mixed with the MTT solution (5 mg/mL, FUJIFILM, Tokyo, Japan). Following 3 h of incubation, the supernatant was removed. The formazan crystals in the cells were then dissolved in DMSO. The amount of formazan dye was measured using an absorbance meter (Benchmark

Table 1. MRM Parameters for Analytes

Analyte	Precursor ion (*m/z*)	Product ion (*m/z*)	Fragmentor voltage (V)	Collision energy (eV)	Polarity
Quercetin	301	151	130	55	—
Myricetin	317	151	130	25	—
Oenothein B	240.1	196.1	250	21	—

Plus microplate spectrophotometer) (Bio-Rad, Hercules, CA, U.S.A.) at a test wavelength of 570 nm and reference wavelength of 630 nm.

Flow Cytometry Analysis Jurkat/Vpr-HiBiT cells were infected with VSV-G-pseudotyped NL4-3/GagVenus cells. At 15 h post-infection, the infected cells were cultured in RPMI1640 with the plant extracts, myricetin, and quercetin to analyze Gag expression for 1 d. The infected cells were fixed with 4% PFA for 30 min. The fluorescence signal (YFP) was analyzed using flow cytometry (FACSCalibur, BD Biosciences, Franklin Lakes, NJ, U.S.A.). To analyze cytotoxicity, Jurkat/Vpr-HiBiT cells were infected with VSV-G-pseudotyped NL4-3/GagVenus. The cells were fixed with 4% PFA for 30 min. Fixed cells were collected and mixed with Annexin V-Cy5 (BD Biosciences) and 7-aminoactinomycin D (7-AAD) (BD Biosciences). After staining, the cells were mixed with actinomycin D (20 μg/mL) (Sigma-Aldrich) and fixed with 1% PFA.[35] Fluorescent signals (Cy5), 7-AAD, and Venus fluorescence were detected in FL4, FL3, and FL1 using flow cytometry (FACSCalibur, BD Biosciences).

Western Blotting Analysis Cells and viruses were lysed with 1% Triton X lysis buffer (50 mM Tris–HCl, pH 7.5, containing 0.5% Triton X-100, 300 mM NaCl, 10 mM iodoacetamide, and a protease inhibitor cocktail (Roche, Basel, Switzerland)). After 2× sodium dodecyl sulfate sample buffer was added, HIV-1 Gag proteins were detected by immunoblotting using an anti-HIV-1 Gag antibody (#24-4) (NIH AIDS Research and Reference Reagent Program) (1 : 1000) as the primary antibody.[36,37] Horseradish peroxidase (HRP)-conjugated anti-mouse immunoglobulin G (IgG) antibody (Bio-Rad) was used as the secondary antibody. Moreover, an HRP-conjugated secondary antibody was detected using ImmunoStar LD (FUJIFILM).

Virus Infectivity Assay Jurkat/Vpr-HiBiT cells were then infected with NL4-3. At 15 h post-infection, cells were treated with the indicated extracts. Three days after infection, the viruses were harvested and precipitated using centrifugation (13200 × ***g***, 60 min at 4 °C) and then resuspended in RPMI1640. The amount of p24 in the viruses was quantified using p24 ELISA. Next, CEM-GFP cells that encode LTR-driven green fluorescent protein (GFP) genes were infected with normalized viruses. Two days post-infection, the infected cells were fixed with 4% PFA. The GFP-positive cell population was analyzed using flow cytometry (FACSCalibur, BD Biosciences).

LC/MS Analysis The analytes, including quercetin, myricetin and oenothein B, were detected by using LC-electrospray ionization-mass spectrometry (ESI-MS) with the Agilent 6460 Triple Quadrupole LC-MS system (Agilent Technologies, Santa Clara, CA, U.S.A.). The LC-tandem mass spectrometry (LC-MS/MS) conditions were described as below: column, YMC-Triart C18 Plus column (2.1 × 50 mm) (YMC Co., Ltd., Kyoto, Japan); column temperature, 45 °C; injection volume, 1 μL; mobile phases: A, 0.1% formic acid, and B, acetonitrile; gradient (B concentration), 0 min–1%, 10 min–80%, 10.1 min–1%, 15 min–1%; and flow rate, 0.2 mL/min. The general conditions for ESI-MS were nebulizer gas, nitrogen, delivered at 50 psi; nebulizer gas temperature, 250 °C; capillary voltage, 3500 V; collision gas, and G1 grade, nitrogen (Taiyo Nippon Sanso Corporation, Tokyo, Japan). Table 1 provides details of the multiple reaction monitoring (MRM) parameters that we used in this study.

RESULTS

Plant Extracts TUR11 and TUR55 from the Library Reduce HIV-1 Release from Host Cells Jurkat/Vpr-HiBiT cells were infected with VSV-G-pseudotyped NL4-3 to identify the extracted plants that would inhibit HIV-1 release from the prepared library of Turkish plants (164 extracts, 50 μg/mL).[31] Because the integration step of HIV-1 is accomplished at 10 h post-infection,[38] the infected cells were treated with these extracted plants at 15 h post-infection to avoid early step inhibition of viral replication. In the first screening, approximately half of the 164 plant extracts were cytotoxic (data not shown). Therefore, these plants were diluted two- or five-fold to reduce cytotoxicity (except for TUR11 and TUR55, which were made up to 25 μg/mL) during the second screening (Fig. 1A). According to the second screening result, 13 extracted plants inhibited the release of Vpr-HiBiT without cytotoxicity (Fig. 1A: blue and red dots). Since Vpr-HiBiT is incorporated into virions, the amount of Vpr-HiBiT indirectly reflects the number of viruses in the cell supernatant. Notably, 5 out of 13 extracted plants showed reduced HIV-1 release based on the three replicate experiments (TUR11, TUR16, TUR22, TUR55, and TUR92) (Fig. 1B, Supplementary Fig. 1). TUR11 and TUR55 inhibited HIV-1 Gag p24 and Vpr-HiBiT in cell supernatants (about 30 and 43% inhibition. TUR92 slightly reduced HIV-1 Gag p24 (about 18% inhibition). Whereas TUR22 reduced the amount of Vpr-HiBiT but not HIV-1 Gag p24 (Fig. 1C). The EC_{50} and CC_{50} were 25 and 76 μg/mL in TUR11 and 15 and 59 μg/mL in TUR55, respectively (Fig. 2). The selectivity index of TUR16 was found to be <1. This result indicates that the reduction in HIV-1 release by TUR16 is caused by cytotoxicity. Coincidentally, only TUR11 and TUR55 belong to the family Onagraceae in the 164 plant extracts, and they were extracted from aerial ingredients (Table 2). Some TUR extracts from aerial ingredients did not significantly inhibit the virus release (Supplementary Figs. 2A, B, Table 3). It suggests that TUR11 and TUR55 may contain inhibitory components against HIV-1 release.

TUR11 and TUR55 Change the Distribution of HIV-1 Gag at the PM HIV-1 Gag binds to and assembles at the PM, and viral particles are formed around the Gag-accumulated locations. Previously, we reported that the mislocalization of Gag by these compounds could trigger apoptosis.[39] To investigate Gag mislocalization by TUR11 and TUR55,

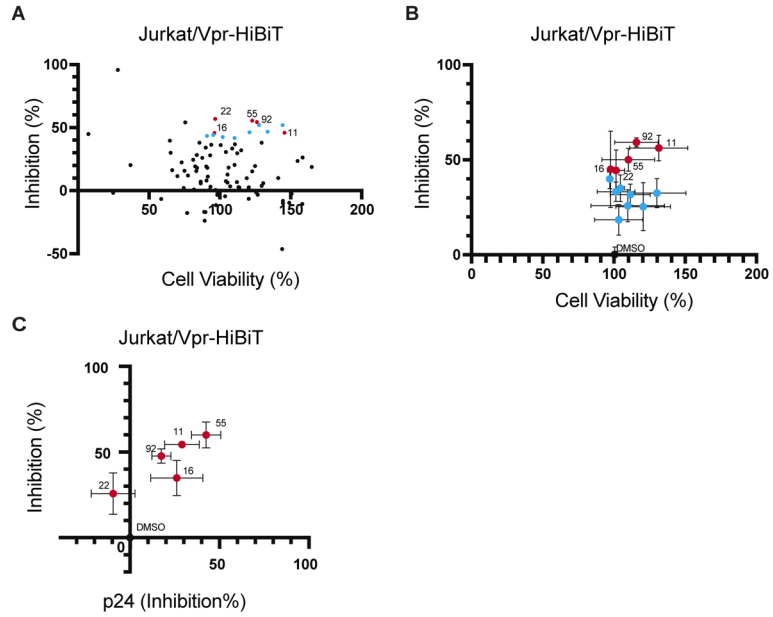


Fig. 1. Five Plant Extracts Were Identified as Candidates for Virus Release Inhibition

(A–C) Jurkat/Vpr-HiBiT cells were infected with VSV-G-pseudotyped-NL4-3/KFS. The infected cells were treated with the plant extracts from the Turkish plant library at 15 h post-infection. The NLuc activity (A–C) and the amount of p24 (C) in the cell supernatants were measured 3 d post-infection. (A, B) The uninfected cells were treated with plant extracts. Two days after treatment with the extracts, the cell viability was examined using MTT assay. The plant extracts in the first screening were shown in light blue dots, and the extracts in the second screening were shown in red dots. The inhibition (%) was calculated as the nanoluciferase values in TUR treatment divided by the nanoluciferase values in dimethyl sulfoxide (DMSO). Data from three independent experiments (B, C) are shown as mean ± standard deviations.

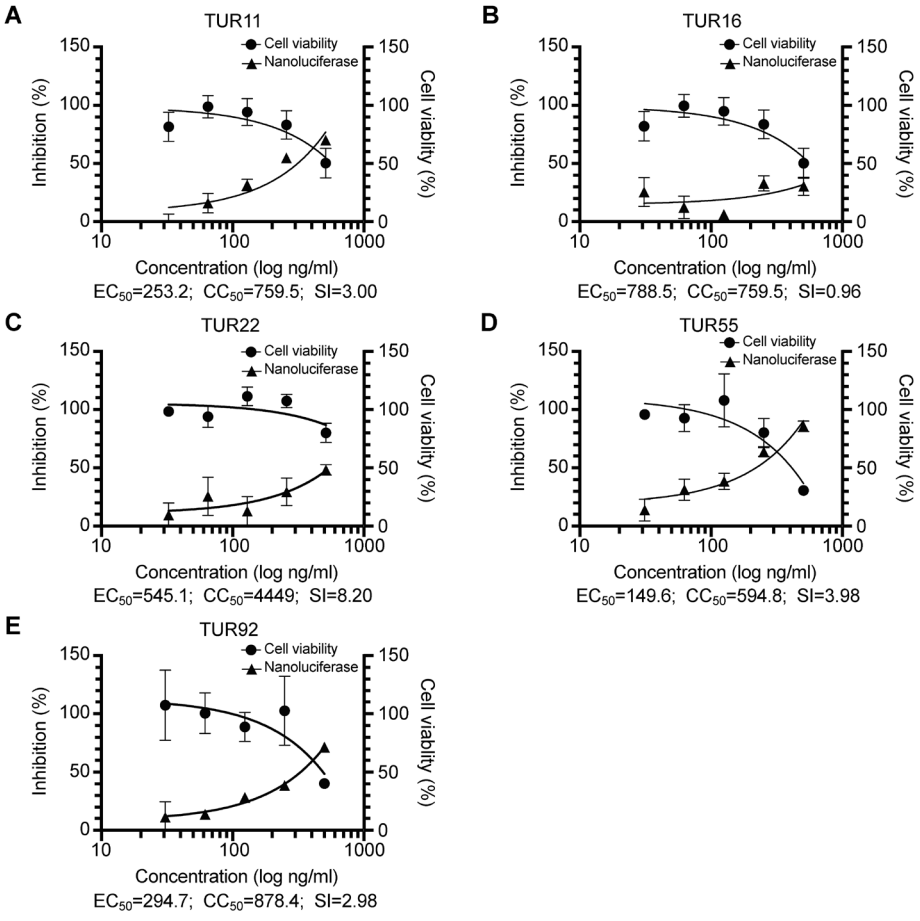


Fig. 2. TUR11 and TUR55 Inhibited Viral Release

Jurkat/Vpr-HiBiT cells were infected with VSV-G-pseudotyped-NL4-3/KFS. The infected cells were treated with the plant extracts at 15 h post-infection. The NLuc activity was measured 3 d post-infection. The uninfected cells were treated with the indicated extracts. Two days after the extract treatment, the cell viability was examined using MTT assay. The inhibition (%) was calculated as the nanoluciferase values in TUR treatment dividing by the nanoluciferase values in DMSO. Prism software was used to determine EC_{50} and CC_{50}. Data from three independent experiments are shown as mean ± standard deviations.

Table 2. Selected Plant Extracts in the Screening System

Name	Scientific name	Order	Family	Genus	Species	Plant part	Yield of extracts
TUR11	*Epilobium hirsutum* L.	Myrtales	Onagraceae	*Epilobium*	*E. hirsutum*	Aerial	2.45%
TUR16	*Eupatorium cannabinum* L.	Asterales	Asteraceae	*Eupatorium*	*E. cannabinum*	Root	3.39%
TUR22	*Rhododendron ponticum* L.	Ericales	Ericaceae	*Rhododendron*	*R. ponticum*	Leaf	7.52%
TUR55	*Chamerion angustifolium* (L.) Holub	Myrtales	Onagraceae	*Chamerion*	*C. angustifolium*	Aerial	14.50%
TUR92	*Senna alexandrina* Mill.	Fabales	Fabaceae	*Senna*	*S. alexandrina*	Leaf	21.80%

Table 3. The Plant Extracts of no Inhibitory Effect in the Screening System

Name	Species	Family	Genus	Plant part	Yield of extracts
	Scientific name				
TUR2	*Fraxinus angustifolia* ssp. *oxycarpa* (M.Bieb. ex Willd.) Franco & Rocha Afonso	Oleaceae	*Fraxinus*	Leaf	6.54%
TUR3-2	*Diospyros lotus* L.	Ebenaceae	*Diospyros*	Fruit	14.32%
TUR11	*Epilobium hirsutum* L.	Onagraceae	*Epilobium*	Aerial	2.45%
TUR16-2	*Eupatorium cannabinum* L.	Compositae	*Eupatorium*	Aerial	4.95%
TUR18	*Ficus carica* L.	Moraceae	*Ficus*	Aerial	4.39%
TUR19-1	*Medicago sativa* L.	Leguminosae	*Medicago*	Aerial	6.74%
TUR31	*Calamintha* sp.	Lamiaceae	*Calamintha*	Aerial	16.71%
TUR41	*Salvia glutinosa* L.	Lamiaceae	*Salvia*	Aerial	6.64%
TUR45-1	*Lycopus europaeus* L.	Lamiaceae	*Lycopus*	Aerial	8.76%
TUR47-1	*Geranium robertianum* L.	Geraniaceae	*Geranium*	Aerial	17.51%
TUR49	*Rhododendron ponticum* L.	Ericaceae	*Rhododendron*	Leaf	0.66%
TUR51-1	*Campanula latifolia* L.	Campanulaceae	*Campanula*	Aerial	3.25%
TUR55	*Chamerion angustifolium* (L.) Holub	Onagraceae	*Chamerion*	Aerial	14.50%
TUR60	*Vicia cracca* L.	Leguminosae	*Vicia*	Aerial	3.45%
TUR61	*Gypsophila silenoides* Rupr.	Caryophyllaceae	*Gypsophila*	Aerial	10.29%
TUR62-1	*Onobrychis arenaria* ssp. *cana* (Boiss.) Hayek	Leguminosae	*Onobrychis*	Aerial	8.83%
TUR64	*Fumaria schleicheri* ssp. *microcarpa* (Hausskn.) Lidén	Papaveraceae	*Fumaria*	Aerial	17.74%
TUR65-1	*Eupatorium cannabinum* L.	Compositae	*Eupatorium*	Stem	11.41%
TUR65-3	*Eupatorium cannabinum* L.	Compositae	*Eupatorium*	Leaf	1.41%
TUR66	*Tilia platyphyllos* Scop.	Malvaceae	*Tilia*	Aerial	10.91%
TUR67	*Thymus* sp. (1)	Lamiaceae	*Thymus*	Aerial	14.93%
TUR69	*Thymus* sp. (2)	Lamiaceae	*Thymus*	Leaf	6.91%
TUR73	*Centaurea cyanus* L.	Compositae	*Centaurea*	Flower	3.75%
TUR74	*Helichrysum arenarium* (L) Moench.	Compositae	*Helichrysum*	Flower	10.39%
TUR75	*Vitex agnus-castus* L.	Lamiaceae	*Vitex*	Fruit	3.70%
TUR76	*Thymus vulgaris* L.	Lamiaceae	*Thymus*	Seed	11.66%
TUR77	*Acer platanoides* L.	Sapindaceae	*Acer*	Aerial	7.40%
TUR78	*Avena sativa* L.	Poaceae	*Avena*	Aerial	9.12%
TUR79	*Thymus* sp. (3)	Lamiaceae	*Thymus*	Aerial	14.14%
TUR88	*Petroselinum crispum* (Mill.) Fuss	Apiaceae	*Petroselinum*	Seed	12.79%
TUR89	*Ceratonia siliqua* L.	Leguminosae	*Ceratonia*	Fruit	15.15%
TUR91	*Glycyrrhiza glabra* L.	Leguminosae	*Glycyrrhiza*	Stem and Bark	25.74%
TUR108	*Boswellia* sp.	Burseraceae	*Boswellia*	Resin	28.73%

we observed the localization of fluorescent-fused Gag using confocal microscopy (Fig. 3A). The cell number, which indicated Gag localization at the PM, was similar for DMSO, TUR11, and TUR55 treatments (Fig. 3B). However, TUR11 and TUR55 disturbed the distribution of HIV-1 Gag at the PM (Fig. 3C). In the DMSO treatment, we observed many Gag puncta at the PM (Figs. 3A, C, Supplementary Fig. 3). The pattern of Gag puncta at the PM of T cells was consistent with a previous report.[9] Compared to DMSO treatment, TUR11 and TUR55 interrupted the formation of Gag punctuation at the PM (Figs. 3A, 3C and Supplementary Fig. 3). It suggests that inhibition of Gag multimerization at the PM inhibits the virus release from the PM.

TUR11 and TUR55 Accelerate the Morphology Changing of HIV-1-Infected Cells To investigate the inhibitory mechanism of TUR11 and TUR55, we measured the amount of HIV-1 Gag in cells and supernatants. Immature Pr55 Gag and mature p24 Gag were detected in cell lysates, and mature p24 Gag was detected in the virus released from infected cells (Fig. 4A). Compared with DMSO treatment, TUR11 and TUR55 reduced about 25% of HIV-1 Pr55 and HIV-1 p24 Gag in both cell and viral lysates (Figs. 4A, B) but not HTLV-1 Gag p24 (Supplementary Figs. 4A–C). The virus release efficiency was calculated as HIV-1 p24 Gag in the viral lysate

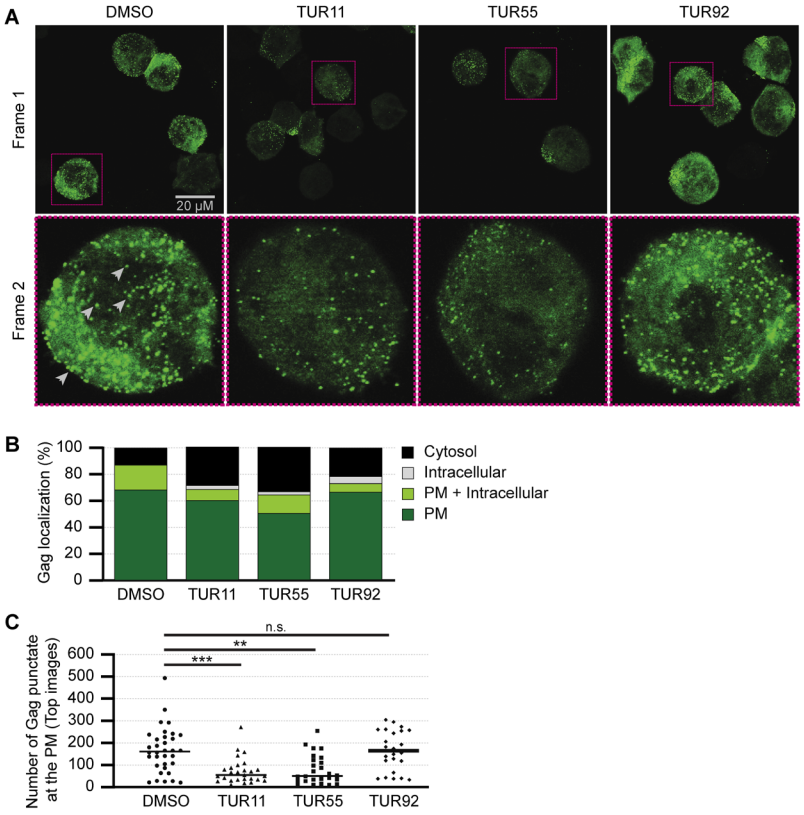


Fig. 3. TUR11 and TUR55 Changed Gag Distribution at the PM

(A–C) Jurkat/Vpr-HiBiT cells were infected with VSV-G-pseudotyped-NL4-3/GagVenus. The infected cells were treated with the indicated extracts at 15 h post-infection. (A) The cells were observed using confocal microscopy. The enlarged images in purple square (frame 1) are shown in frame 2. Gray arrows indicate the representative punctuate at the PM. (B) The cells with Gag localized predominantly to the PM (dark green), both PM and intracellular compartments (light green), the intracellular compartments (gray), or the cytosol (black) were counted. Approximately 100 cells that showed Gag signals were examined. (C) The number of Gag punctate at the PM were counted using ImageJ and analyzed using Prism 9 software. *p*-Values were determined with Student's *t* test. $^{**}p < 0.001$; $^{***}p < 0.0001$; *n.s.*, not significant.

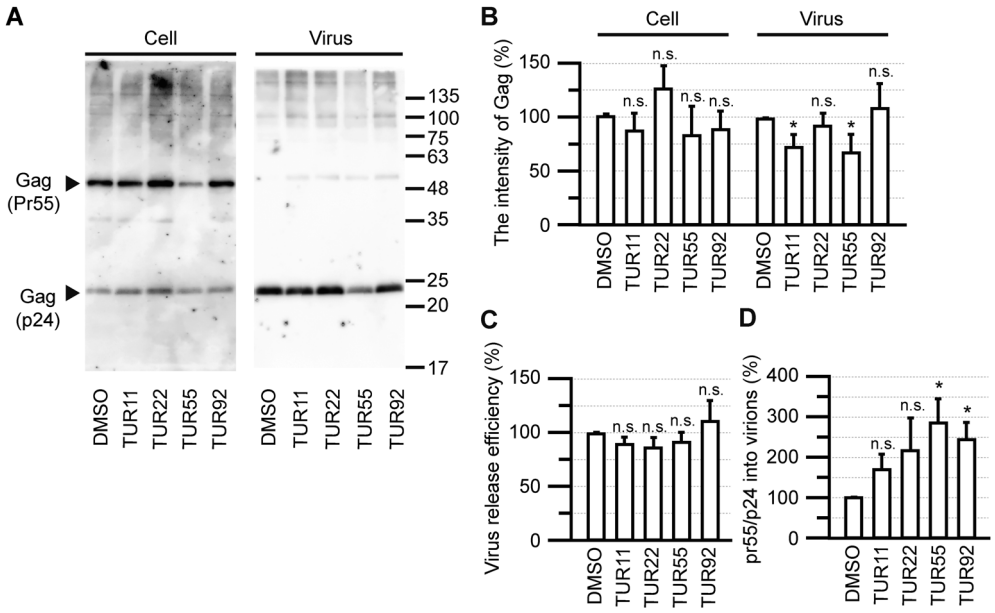


Fig. 4. Human Immunodeficiency Virus (HIV)-1 Gag Expression Was Reduced in TUR11 and TUR55 Treated T Cells

(A) Jurkat/Vpr-HiBiT cells were infected with VSV-G-pseudotyped-NL4-3/KFS. The infected cells were treated with the plant extracts at 15 h post-infection. Three days after infection, the amount of HIV-1 Gag was measured with Western blotting. (B) The intensity of Gag (Pr55 and p24) was measured using ImageJ software. (C) The virus release efficiency was calculated as the amount of virion-associated Gag as a fraction of the total amount of Gag. (D) The ratio of immature Gag was calculated as the amount of virion-associated Pr55 as a fraction of the virion-associated of total Gag (Pr55 and p24). Data from three independent experiments (B–D) are shown as mean ± standard deviation. *p*-Values were determined with Student's *t* test. $^{*}p < 0.01$; *n.s.*, not significant.

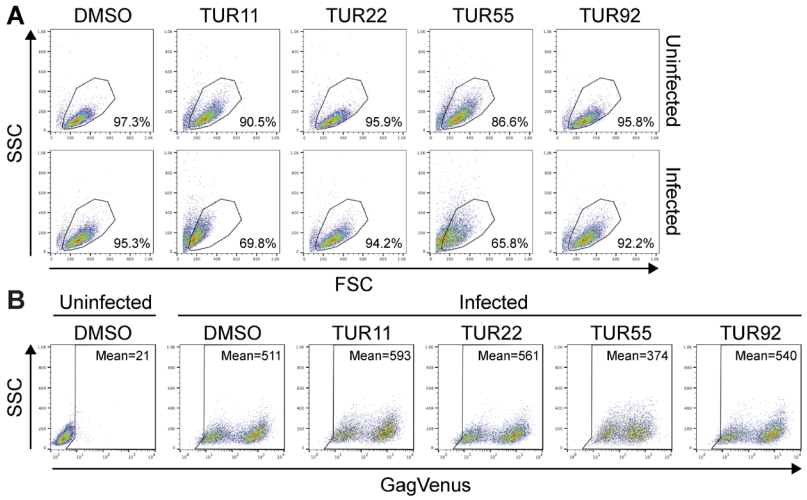


Fig. 5. TUR11 and TUR55 Changed the Morphology of HIV-1-Infected Cells

(A–D) Jurkat/Vpr-HiBiT cells were treated with the indicated extracts. (A, B) Jurkat/Vpr-HiBiT cells were infected with VSV-G-pseudotyped-NL4-3/GagVenus. (A) The size and granularity of cells were analyzed by forward scatter (FSC) and side scatter (SSC). The percentage indicates the number of cell population in the gated regions. (B) The fluorescence intensity of GagVenus was detected by FL1. The mean indicates the fluorescence intensity of GagVenus in the gated regions.

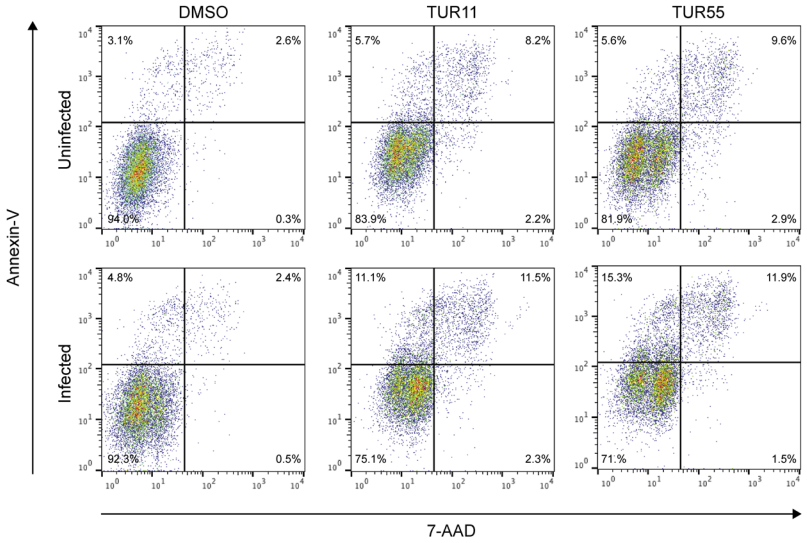


Fig. 6. TUR11 and TUR55 Increased the Number of Annexin-Positive Cells in HIV-1-Infected Cells

The uninfected Jurkat/Vpr-HiBiT cells were treated with the indicated extracts (Upper panels). Jurkat/Vpr-HiBiT cells were infected with VSV-G-pseudotyped-NL4-3/GagVenus, and then were treated with the indicated extracts (Lower panels). Two days after extract treatments, the infected cells were stained with Annexin V and 7-AAD. The percentage indicates the number of cell population in the gated regions.

divided by the total Gag in both the cell and virus lysates. The results showed that the viral release efficiency was similar between the DMSO- and extract-treated plants (Fig. 4C). This result indicates that TUR11 and TUR55 may inhibit the synthesis of HIV-1 Gag proteins or induce the degradation of HIV-1 Gag. Otherwise, TUR11 and TUR55 might accelerate cell death *via* the cytotoxicity pathway, as reported previously.[39] Notably, the amounts of Pr55 relative to the p24 into virions were increased by the TUR55 and TUR92 treatments (Figs. 4A, D). It suggests that TUR55 and TUR92 interrupt the virus maturation in the alternative pathway.

To clarify whether TUR11 and TUR55 degrade the amounts of Gag in cells, we examine the fluorescent intensity of Gag in cells using flow cytometry. The size and granularity of cells were similar between DMSO and extracted plants (DMSO; 97.3%, TUR11; 90.5%, TUR55; 86.6%) (Fig. 5A, upper panels). However, in HIV-1-infected cells, the size and granularity of infected cells were altered by TUR11 and TUR55, and about 30% of cell populations were shifted outside the gate. (Fig. 5A, lower panels). These results indicate that TUR11 and TUR55 accelerated the altering of infected-cell morphology. As a result, the total amount of HIV-1 Gag would be reduced (Figs. 4A, B). On the other hand, the mean fluorescence intensity of HIV-1 Gag in the gated-cell population (Fig. 5A, lower panels) was 27% reduced by TUR55 but not TUR11 (Fig. 5B). It suggests that the inhibition of HIV-1 release accelerates the cell-death rather than the accumulation of HIV-1 Gag in the cells.

TUR11, TUR55, Quercetin, and Oenothein B Induce the Infected-Cell Death *via* the Apoptotic Pathway To clarify whether TUR11 and TUR55 induce the cell death in the apoptotic pathway, the cells were stained with the apoptosis markers annexin V and 7-AAD at 48 h post-infection (Fig. 6). TUR11 and TUR55 increased the population of annexin-

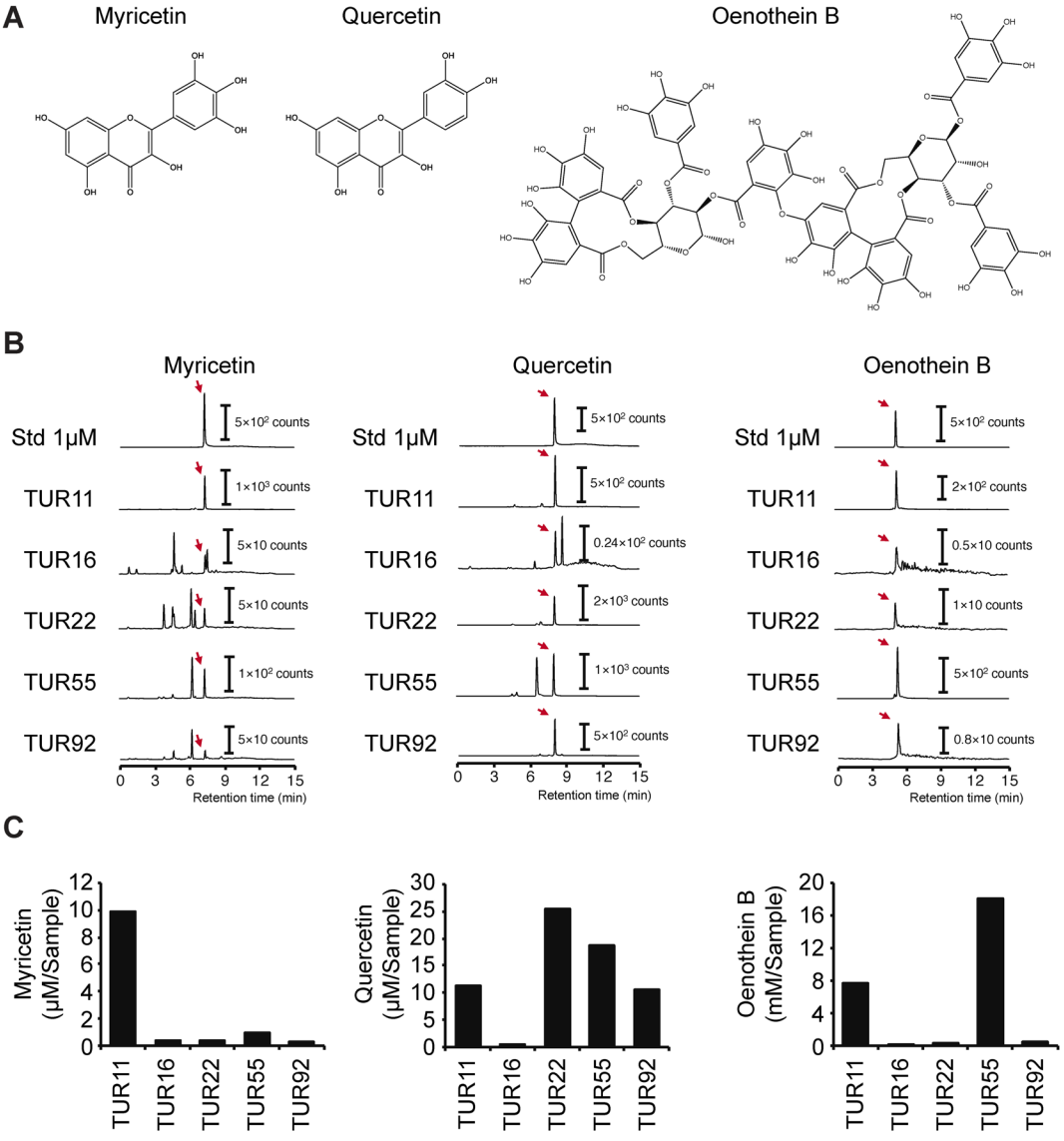


Fig. 7. The Myricetin, Quercetin, and Oenothein B Are Components in the TUR11 and TUR55

(A) The structures of myricetin and quercetin, and oenothein B. (B) Chromatography of analytes from extractions. Peaks with corresponding MRM indicate the quercetin, myricetin and oenothein B (red arrows), respectively. (C) The concentrations of quercetin, myricetin and oenothein B in the extractions were measured by means of LC-MS/MS. The 1/200 amounts of each extract were used for the experiments.

positive cells in the HIV-1-infected cells (Fig. 6, lower panels). It suggests that TUR11 and TUR55 accelerate cell death *via* a cell apoptotic pathway in the HIV-1-infected cells.

According to a previous report, *Epilobium hirsutum* L., which is the same family as TUR11 and TUR55, primarily contains oenothein B, myricetin and quercetin[40] (Fig. 7A). Thus, we measured the amounts of each component using LC/MS (Figs. 7B, C, Supplementary Fig. 5). The large amount of oenothein B and the small amount of myricetin and quercetin were detected in TUR11 and TUR55. We evaluated these chemical components' inhibitory effects on HIV-1 release. The oenothein B (100 μM) showed cell cytotoxicity in uninfected cells, and the oenothein B (50 μM) only 20% reduced the virus release and did not change the number of Gag punctate at PM (Figs. 8A–D). The myricetin (20 μM) and quercetin (20 μM) showed less cell cytotoxicity and approximately 50% virus release inhibition (Figs. 8A, B). The lower amounts of myricetin (10 and 5 μM) and quercetin (10 μM) significantly reduced the viral release (Supplementary Figs. 6A, B). The myricetin and quercetin reduced the number of Gag punctate at the PM (Figs. 8C, D). The myricetin and quercetin further increased the population of annexin-positive cells, although the myricetin induced 30–50% cytotoxic cells even in the uninfected cells (Fig. 8E). Notably, TUR11, TUR55, and quercetin have lower cell-cytotoxicity than myricetin at the earlier time (8 h), but they have a similar HIV-1-inhibitory activity (Figs. 8B, E). To investigate the synergistically effect of quercetin and oenothein B, the cell viability and HIV-1 release inhibition were examined in a dose-dependent manner (Figs. 9A, B). The quercetin with oenothein B further inhibited the HIV-1 release (Fig. 9B). Importantly, in the presence of oenothein B (50 μM), a small amount of quercetin (0.08 μM) 40% reduced the HIV-1 release. Taken together, quercetin inhibits the virus release and accelerates cell death *via* a cell apoptotic pathway, and oenothein B synergistically inhibits the virus release.

TUR55 and TUR92 Reduce the Infectivity of HIV-1 As TUR11 and TUR55 might interrupt Gag multimerization, abnormal virions might be formed by the disorganized Gag as-

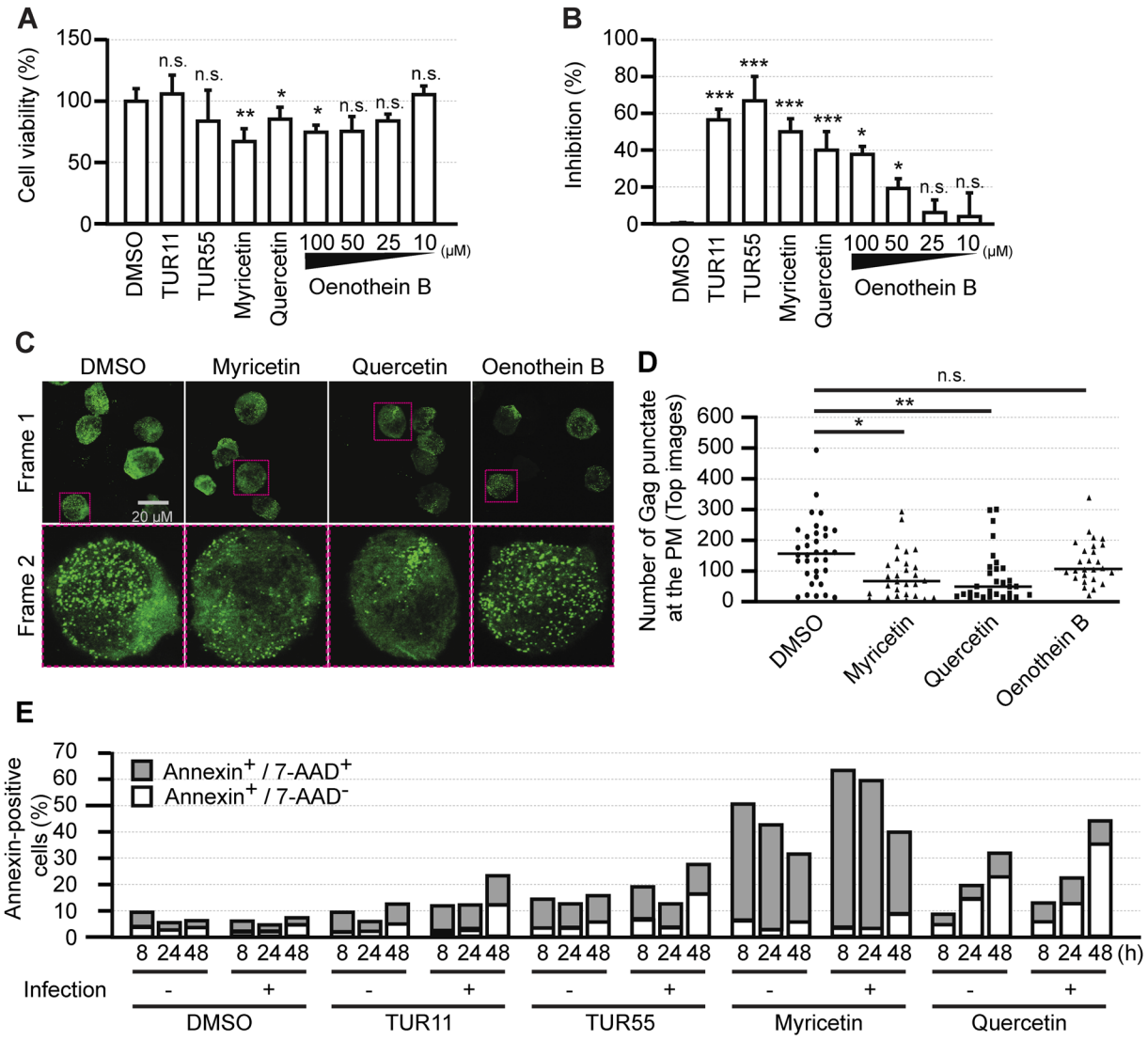


Fig. 8. The Quercetin Increased the Number of Annexin-Positive Cells

(A) The uninfected cells were treated with the indicated compounds. Two days after the extract treatment, the cell viability was examined using MTT assay. (B) Jurkat/Vpr-HiBiT cells were infected with VSV-G-pseudotyped-NL4-3/KFS. The infected cells were treated with the plant extracts, myricetin, quercetin, and oenothein B at 15 h post-infection. The NLuc activity was measured 3 d post-infection. The inhibition (%) was calculated as the nanoluciferase values in compounds treatment dividing by the nanoluciferase values in DMSO. Data from three independent experiments (A, B) are shown as mean ± standard deviation. *p*-Values were determined with Student's *t* test. $*p<0.01$; $**p<0.001$; $***p<0.0001$; *n.s.*, not significant. (C) The cells were observed using confocal microscopy. The enlarged images in purple square (frame 1) are shown in frame 2. (D) The number of Gag punctate at the PM were counted using ImageJ and analyzed using Prism 9 software. *p* values were determined with Student's *t* test. $*p<0.01$; $**p<0.001$. (E) Jurkat/Vpr-HiBiT cells were infected with VSV-G-pseudotyped-NL4-3/GagVenus. The infected cells were treated with the plant extracts, myricetin and quercetin at 15 h post-infection. The infected cells were stained with Annexin V and 7-AAD at 8, 24, 48 h post-treatments. The number of annexin-positive cells were quantified using flow cytometry analysis.

sembly at the PM. Therefore, TUR11 and TUR55 may reduce the infectivity of progeny viruses. Thus, we harvested viruses from producer cells treated with plant extracts and concentrated the viruses using centrifugation to remove the carry-on of the plant extracts from the harvested viruses. The amount of harvested virus was normalized to the amount of p24 Gag. CEM-GFP cells were infected with the same amounts of viruses (Figs. 10A, B). HIV-1 Tat drives GFP-reporter genes in infected CEM-GFP cells. TUR55 markedly reduced the infectivity of viruses, but not TUR11, suggesting that compared to TUR11, TUR55 might have a different inhibitory mechanism. Unexpectedly, TUR92 reduced viral infectivity without affecting virus release. This result indicates that TUR55 and TUR92 might contains the other important constituents to reduce viral infectivity *via* an alternative pathway. The viral infectivity might be decreased by the inhibition of virus maturation (Fig. 4D). It suggests that TUR55 synergistically inhibits the viral replication by the inhibition of virus release and infectivity.

DISCUSSION

In this study, we discovered that candidate plant extracts TUR11 and TUR55 from our original plant library inhibit HIV-1 release. HIV-1 Gag at the PM was dispersed and distributed throughout the cell surface in the presence of TUR11 and TUR55. These extracts accelerated the cell apoptosis in HIV-1-infected cells. Quercetin and oenothein B, are chemical components in *Chamerion angustifolium* (L.) Holub, are crucial for the inhibition of the HIV-1 release. Moreover, the infectivity of the progeny virus from TUR55-treated cells was reduced through different inhibitory mechanisms.

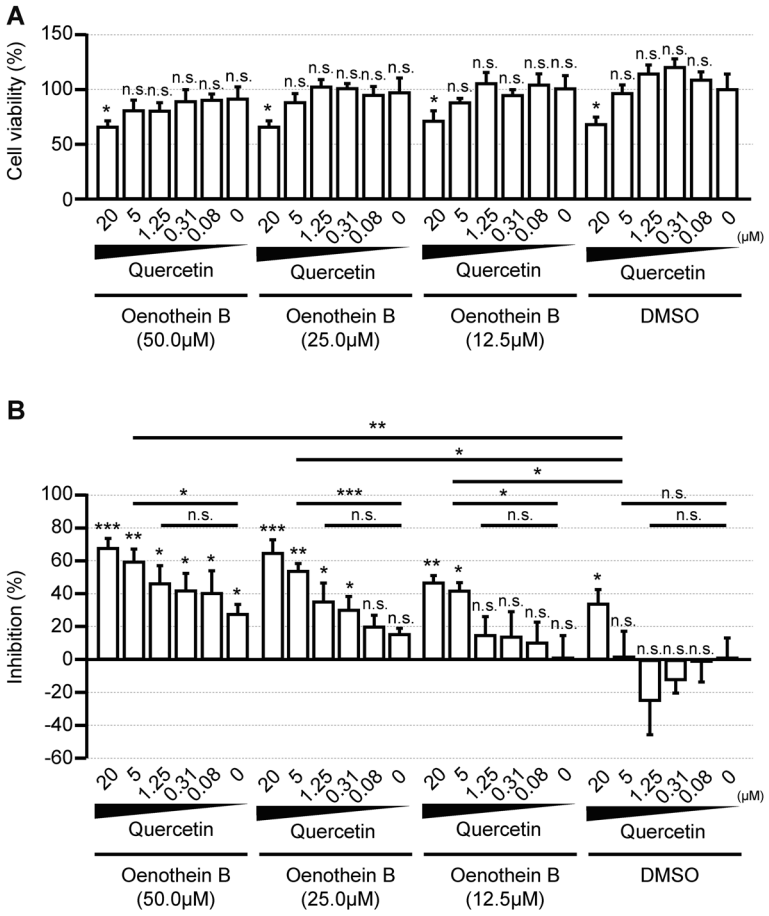


Fig. 9. The Oenothein B Synergistically Inhibited the HIV-1 Release

(A) The uninfected cells were treated with the quercetin and oenothein B. Two days after the extract treatment, the cell viability was examined using MTT assay. (B) Jurkat/Vpr-HiBiT cells were infected with VSV-G-pseudotyped-NL4-3/KFS. The infected cells were treated with quercetin and oenothein B at 15 h post-infection. The NLuc activity was measured 3 d post-infection. The inhibition (%) was calculated as the nanoluciferase values in compounds treatment dividing by the nanoluciferase values in DMSO. Data from three independent experiments (A, B) are shown as mean ± standard deviation. *p*-Values were determined with Student's *t* test. $*p<0.01$; $**p<0.001$; $***p<0.0001$; *n.s.*, not significant.

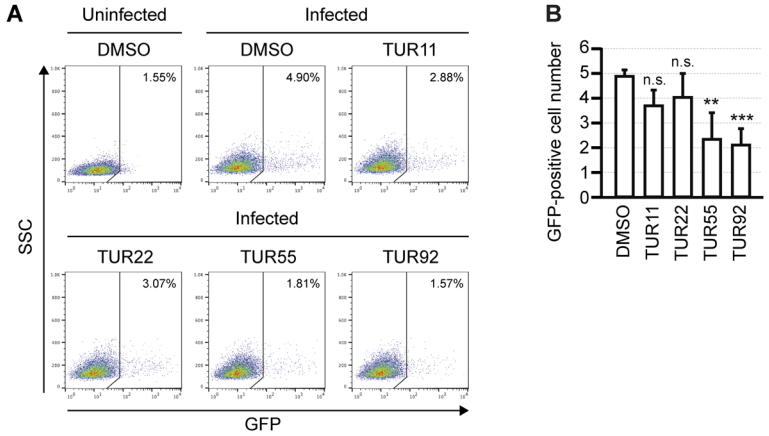


Fig. 10. TUR55 and TUR92 Reduced the Progeny Viral Infectivity

(A) Jurkat/Vpr-HiBiT cells were infected with NL4-3. The cells were treated with the indicated extracts. Three days after infection, the viruses were harvested and normalized by the amount of p24. The CEM-GFP cells were infected with the normalized viruses, and the GFP-positive cell population was analyzed using flow cytometry. (B) The average of GFP-positive cell in three independent experiments were calculated. Data from three independent experiments are shown as mean ± standard deviation. *p*-Values were determined with Student's *t* test. $**p<0.001$; $***p<0.0001$; *n.s.*, not significant.

Using the total number of plant extracts, we found that TUR11 and TUR55 inhibited HIV-1 release in T cells. These plants belong to the same family (Onagraceae), suggesting they may contain similar components. Zengin *et al.* characterized the components of *E. hirsutum* (Onagraceae) in the aerial parts and roots.[40] Accordingly, oenothein B is one of the components of *E. hirsutum*. Oenothein B isomer, a major component of macrocyclic ellagitannin, has been purified from food plants such as *E. angustifolium*.[41–43] Oenothein B has broad biological activities, including antioxidant,[44] anti-inflamma-

tory,[45,46] antitumor,[47–49] and antiviral (against hepatitis C) activities.[50] Notably, oenothein B induces cell apoptosis *via* the reactive oxygen species (ROS)-mediated phosphatidylinositol 3-kinase (PI3K)/protein kinase B (Akt)/nuclear factor-kappa B (NF-κB) signaling pathway.[49] HIV-1 infection activates the PI3K/Akt/NF-κB signaling pathway[51] for several cellular processes, such as cell survival and metabolism, involved in HIV-1 pathogenesis.[52] In this study, oenothein B (100 μM) induced cell cytotoxicity in uninfected-Jurkat T cells (Fig. 8A). Because oenothein B has antitumor activity, immortalized cell lines such as Jurkat T cells might die by cell apoptosis. On the other hand, myricetin and quercetin inhibit the HIV-1 reverse transcription at the early step.[53–56] However, the inhibitory mechanism at the late step of HIV-1 replication was not evaluated. Significantly, flavonoids induce apoptosis in several cancer cells through modulation of Foxo3a activity.[57] Quercetin, which is one of the flavonoids, might accelerate the cell-apoptosis in HIV-1-infected cells through a similar modulation. However, quercetin is broadly contained in several plants. It is not clear why the quercetin included in only TUR11 and TUR55 accelerated the cell apoptosis in HIV-1-infected cells. We speculate that oenothein B in TUR11 and TUR55 might contribute to the anti-viral effect of quercetin at the late stage, then quercetin might kill the Gag-accumulated cells. In the future, we should further investigate the inhibitory mechanisms of HIV-1 Gag assembly by mixing oenothein B and quercetin.

The infectivity of the progeny virus produced from TUR55-treated T cells was reduced; however, it was found that TUR11 did not affect infectivity. According to the flow cytometry analysis results, the signal intensity of Gag in the cells was different between the TUR11 and TUR55 treatments (Fig. 5B). These results suggested that Gag might be degraded TUR55-treated cells. The association between Gag degradation and viral infectivity is unclear; however, different components of TUR11 and TUR55 may play a role in alternative inhibition. Unexpectedly, TUR92, ruled out as a viral release inhibitor, markedly reduced viral infectivity, similar to TUR55. TUR55 and TUR92 likely interrupted the processing of immature Gag Pr55 and the forming of the core in the viral particles (Fig. 4D). TUR92, a member of the Fabaceae family (*Senna alexandrina* Mill.), has been used in various laxatives. One of the components of *C. angustifolia* Vahl is sennosides,[58] which inhibit HIV-1 infectivity by targeting reverse transcription.[59] Consistently, the accurate forming of viral core at the maturation step is essential for the reverse transcription,[60–65] suggesting that TUR92 may inhibit reverse transcriptase. Further study of the inhibitory mechanisms of TUR55 and TUR92 is necessary to determine their potential as novel HIV-1 drugs.

Some natural products have been discovered, and synthetic analogs have been developed for HIV-1 suppression.[20,21] However, no drugs are currently on the market which are derived from natural sources. Bevirimat (PA-457), a well-known synthetic analog of betulinic acid, has reached phase IIb clinical trials.[26,27] However, the clinical trial was halted due to loss of susceptibility.[30,66] The terpenoid betulinic acid is a component of *Syzygium claviflorum* leaves.[67] In this study, we discovered candidate plant extracts using our screening system, which were active as anti-HIV-1 inhibitors. However, we should purify the components from these candidate plant extracts and investigate the inhibitory effects in future studies. The components that kill the infected cells might serve in the "shock and kill strategy" using a latency-reversing agent. Therefore, using natural compounds against HIV-1 is still a worthwhile avenue for discovering new drugs.

Acknowledgments We would like to thank Dr. E. Freed for providing plasmids, and Dr. Jacques Corbeil for providing the CEM-GFP cells.

This work was supported by AMED (21fk0410026h0001) to K.M., JSPS KAKENHI (19K23802) to H.T., and the Young Investigator Award at the Joint Research Center for Human Retrovirus Infection, Kumamoto University to K.M., and The Shinnihon Foundation of Advanced Medical Treatment Research to K.M., and Bilateral Joint Research Project from the Japan Society for the Promotion of Science (16039901-00867) to M.O., and a Grant in Aid for Scientific Research (B) from the Japan Society for the Promotion of Science (20H03365) to M.F.

Author Contributions KM, MF, TW, YM, HT, and TS conceived of and coordinated the study. YT, AT, PN, HT, NM, JK and WA performed experiments. KM established the cell lines for drug screening. TW, DA, MW, KS, SG, HC, NS, FK collected the plants and prepared a plant library. TZ and DW performed LC/MS analysis. All the authors have read and approved the final manuscript.

Conflict of Interest The authors declare no conflict of interest.

Supplementary Materials This article contains supplementary materials.

REFERENCES

1) Deeks SG, Lewin SR, Havlir DV. The end of AIDS: HIV infection as a chronic disease. *Lancet*, **382**, 1525–1533 (2013).
2) Zhang X. Anti-retroviral drugs: current state and development in the next decade. *Acta Pharm. Sin. B*, **8**, 131–136 (2018).
3) Dick A, Cocklin S. Recent advances in HIV-1 gag inhibitor design and development. *Molecules*, **25**, 1687 (2020).
4) Adamson CS, Freed EO. Human immunodeficiency virus type 1 assembly, release, and maturation. *Adv. Pharmacol.*, **55**, 347–387 (2007).
5) Freed EO. HIV-1 assembly, release and maturation. *Nat. Rev. Microbiol.*, **13**, 484–496 (2015).
6) Bell NM, Lever AM. HIV Gag polyprotein: processing and early viral particle assembly. *Trends Microbiol.*, **21**, 136–144 (2013).
7) Tang C, Loeliger E, Luncsford P, Kinde I, Beckett D, Summers MF. Entropic switch regulates myristate exposure in the HIV-1 matrix protein. *Proc. Natl. Acad. Sci. U.S.A.*, **101**, 517–522 (2004).
8) Chukkapalli V, Hogue IB, Boyko V, Hu WS, Ono A. Interaction between the human immunodeficiency virus type 1 Gag matrix domain and phosphatidylinositol-(4,5)-bisphosphate is essential for efficient gag membrane binding. *J. Virol.*, **82**, 2405–2417 (2008).
9) Monde K, Chukkapalli V, Ono A. Assembly and replication of HIV-1 in T cells with low levels of phosphatidylinositol-(4,5)-bisphosphate. *J. Virol.*, **85**, 3584–3595 (2011).
10) Hill CP, Worthylake D, Bancroft DP, Christensen AM, Sundquist WI. Crystal structures of the trimeric human immunodeficiency virus type 1 matrix protein: implications for membrane association and assembly. *Proc. Natl. Acad. Sci. U.S.A.*, **93**, 3099–3104 (1996).
11) Checkley MA, Luttge BG, Freed EO. HIV-1 envelope glycoprotein biosynthesis, trafficking, and incorporation. *J. Mol. Biol.*, **410**,

582–608 (2011).
12) Tedbury PR, Ablan SD, Freed EO. Global rescue of defects in HIV-1 envelope glycoprotein incorporation: implications for matrix structure. *PLoS Pathog.*, **9**, e1003739 (2013).
13) Briggs JA, Riches JD, Glass B, Bartonova V, Zanetti G, Krausslich HG. Structure and assembly of immature HIV. *Proc. Natl. Acad. Sci. U.S.A.*, **106**, 11090–11095 (2009).
14) Wright ER, Schooler JB, Ding HJ, Kieffer C, Fillmore C, Sundquist WI, Jensen GJ. Electron cryotomography of immature HIV-1 virions reveals the structure of the CA and SP1 Gag shells. *EMBO J.*, **26**, 2218–2226 (2007).
15) Accola MA, Ohagen A, Gottlinger HG. Isolation of human immunodeficiency virus type 1 cores: retention of Vpr in the absence of p6(gag). *J. Virol.*, **74**, 6198–6202 (2000).
16) Levin JG, Guo J, Rouzina I, Musier-Forsyth K. Nucleic acid chaperone activity of HIV-1 nucleocapsid protein: critical role in reverse transcription and molecular mechanism. *Prog. Nucleic Acid Res. Mol. Biol.*, **80**, 217–286 (2005).
17) Morita E, Sandrin V, McCullough J, Katsuyama A, Baci Hamilton I, Sundquist WI. ESCRT-III protein requirements for HIV-1 budding. *Cell Host Microbe*, **9**, 235–242 (2011).
18) Paxton W, Connor RI, Landau NR. Incorporation of Vpr into human immunodeficiency virus type 1 virions: requirement for the p6 region of gag and mutational analysis. *J. Virol.*, **67**, 7229–7237 (1993).
19) Hassan Khan MT, Ather A. Potentials of phenolic molecules of natural origin and their derivatives as anti-HIV agents. *Biotechnol. Annu. Rev.*, **13**, 223–264 (2007).
20) Andersen RJ, Ntie-Kang F, Tietjen I. Natural product-derived compounds in HIV suppression, remission, and eradication strategies. *Antiviral Res.*, **158**, 63–77 (2018).
21) Popović-Djordjević J, Quispe C, Giordo R, Kostić A, Katanic Stanković JS, Tsouh Fokou PV, Carbone K, Martorell M, Kumar M, Pintus G, Sharifi-Rad J, Docea AO, Calina D. Natural products and synthetic analogues against HIV: a perspective to develop new potential anti-HIV drugs. *Eur. J. Med. Chem.*, **233**, 114217 (2022).
22) Mazalovska M, Kouokam JC. Lectins as promising therapeutics for the prevention and treatment of HIV and other potential coinfections. *Biomed. Res. Int.*, **2018**, 3750646 (2018).
23) Akkouh O, Ng TB, Singh SS, Yin C, Dan X, Chan YS, Pan W, Cheung RC. Lectins with anti-HIV activity: a review. *Molecules*, **20**, 648–668 (2015).
24) Liu YP, Yan G, Xie YT, Lin TC, Zhang W, Li J, Wu YJ, Zhou JY, Fu YH. Bioactive prenylated coumarins as potential anti-inflammatory and anti-HIV agents from Clausena lenis. *Bioorg. Chem.*, **97**, 103699 (2020).
25) Otsuki K, Li W, Asada Y, Chen CH, Lee KH, Koike K. Daphneodorins A-C, anti-HIV gnidimacrin related macrocyclic daphnane orthoesters from *Daphne odora*. *Org. Lett.*, **22**, 11–15 (2020).
26) Li F, Goila-Gaur R, Salzwedel K, Kilgore NR, Reddick M, Matallana C, Castillo A, Zoumplis D, Martin DE, Orenstein JM, Allaway GP, Freed EO, Wild CT. PA-457: a potent HIV inhibitor that disrupts core condensation by targeting a late step in Gag processing. *Proc. Natl. Acad. Sci. U.S.A.*, **100**, 13555–13560 (2003).
27) Smith PF, Ogundele A, Forrest A, Wilton J, Salzwedel K, Doto J, Allaway GP, Martin DE. Phase I and II study of the safety, virologic effect, and pharmacokinetics/pharmacodynamics of single-dose 3-o-(3′,3′-dimethylsuccinyl)betulinic acid (bevirimat) against human immunodeficiency virus infection. *Antimicrob. Agents Chemother.*, **51**, 3574–3581 (2007).
28) Martin DE, Blum R, Doto J, Galbraith H, Ballow C. Multiple-dose pharmacokinetics and safety of bevirimat, a novel inhibitor of HIV maturation, in healthy volunteers. *Clin. Pharmacokinet.*, **46**, 589–598 (2007).
29) Adamson CS, Sakalian M, Salzwedel K, Freed EO. Polymorphisms in Gag spacer peptide 1 confer varying levels of resistance to the HIV- 1 maturation inhibitor bevirimat. *Retrovirology*, **7**, 36 (2010).
30) Van Baelen K, Salzwedel K, Rondelez E, Van Eygen V, De Vos S, Verheyen A, Steegen K, Verlinden Y, Allaway GP, Stuyver LJ. Susceptibility of human immunodeficiency virus type 1 to the maturation inhibitor bevirimat is modulated by baseline polymorphisms in Gag spacer peptide 1. *Antimicrob. Agents Chemother.*, **53**, 2185–2188 (2009).
31) Shida W, Tateishi H, Tahara Y, Fujita M, Husham Majeed Alsaadi D, Watanabe M, Koga R, Radwan MO, Ciftci HI, Gezici S, Kurauchi Y, Katsuki H, Otsuka M, Sugimura K, Wada M, Sekeroglu N, Watanabe T. Antileukemic activity of twig components of Caucasian beech in Turkey. *Molecules*, **24**, 3850 (2019).
32) Freed EO, Englund G, Martin MA. Role of the basic domain of human immunodeficiency virus type 1 matrix in macrophage infection. *J. Virol.*, **69**, 3949–3954 (1995).
33) Gervaix A, West D, Leoni LM, Richman DD, Wong-Staal F, Corbeil J. A new reporter cell line to monitor HIV infection and drug susceptibility *in vitro*. *Proc. Natl. Acad. Sci. U.S.A.*, **94**, 4653–4658 (1997).
34) Ono A, Freed EO. Plasma membrane rafts play a critical role in HIV-1 assembly and release. *Proc. Natl. Acad. Sci. U.S.A.*, **98**, 13925–13930 (2001).
35) Schmid I, Uittenbogaart CH, Keld B, Giorgi JV. A rapid method for measuring apoptosis and dual-color immunofluorescence by single laser flow cytometry. *J. Immunol. Methods*, **170**, 145–157 (1994).
36) Simon JH, Fouchier RA, Southerling TE, Guerra CB, Grant CK, Malim MH. The Vif and Gag proteins of human immunodeficiency virus type 1 colocalize in infected human T cells. *J. Virol.*, **71**, 5259–5267 (1997).
37) Fouchier RA, Meyer BE, Simon JH, Fischer U, Malim MH. HIV-1 infection of non-dividing cells: evidence that the amino-terminal basic region of the viral matrix protein is important for Gag processing but not for post-entry nuclear import. *EMBO J.*, **16**, 4531–4539 (1997).
38) Burdick RC, Li C, Munshi M, Rawson JMO, Nagashima K, Hu WS, Pathak VK. HIV-1 uncoats in the nucleus near sites of integration. *Proc. Natl. Acad. Sci. U.S.A.*, **117**, 5486–5493 (2020).
39) Tateishi H, Monde K, Anraku K, Koga R, Hayashi Y, Ciftci HI, DeMirci H, Higashi T, Motoyama K, Arima H, Otsuka M, Fujita M. A clue to unprecedented strategy to HIV eradication: "Lock-in and apoptosis". *Sci. Rep.*, **7**, 8957 (2017).
40) Ak G, Zengin G, Mahomoodally MF, Llorent-Martinez E, Orlando G, Chiavaroli A, Brunetti L, Recinella L, Leone S, Di Simone SC, Menghini L, Ferrante C. Shedding light into the connection between chemical components and biological effects of extracts from Epilobium hirsutum: is it a potent source of bioactive agents from natural treasure? *Antioxidants* (Basel), **10**, 1389 (2021).
41) Ruszová E, Cheel J, Pávek S, Moravcová M, Hermannová M, Matějková I, Spilková J, Velebny V, Kubala L. Epilobium angustifolium extract demonstrates multiple effects on dermal fibroblasts *in vitro* and skin photo-protection *in vivo*. *Gen. Physiol. Biophys.*, **32**, 347–359 (2013).
42) Kaškonienė V, Stankevičius M, Drevinskas T, Akuneca I, Kaškonas P, Bimbiraitė-Survilienė K, Maruška A, Ragažinskienė O, Kornyšova O, Briedis V, Ugenskienė R. Evaluation of phytochemical composition of fresh and dried raw material of introduced Chamerion angustifolium L. using chromatographic, spectrophotometric and chemometric techniques. *Phytochemistry*, **115**, 184–193 (2015).
43) Vitalone A, McColl J, Thome D, Costa LG, Tita B. Characterization of the effect of Epilobium extracts on human cell proliferation. *Pharmacology*, **69**, 79–87 (2003).
44) Li W, Li Z, Peng MJ, Zhang X, Chen Y, Yang YY, Zhai XX, Liu G, Cao Y. Oenothein B boosts antioxidant capacity and supports metabolic pathways that regulate antioxidant defense in *Caenorhabditis elegans*. *Food. Funct.*, **11**, 9157–9167 (2020).
45) Kiss AK, Bazylko A, Filipek A, Granica S, Jaszewska E, Kiarszys

U, Kosmider A, Piwowarski J. Oenothein B's contribution to the anti-inflammatory and antioxidant activity of *Epilobium* sp. *Phytomedicine*, **18**, 557–560 (2011).
46) Okuyama S, Makihata N, Yoshimura M, Amakura Y, Yoshida T, Nakajima M, Furukawa Y. Oenothein B suppresses lipopolysaccharide (LPS)-induced inflammation in the mouse brain. *Int. J. Mol. Sci.*, **14**, 9767–9778 (2013).
47) Miyamoto K, Nomura M, Sasakura M, Matsui E, Koshiura R, Murayama T, Furukawa T, Hatano T, Yoshida T, Okuda T. Antitumor activity of oenothein B, a unique macrocyclic ellagitannin. *Jpn. J. Cancer Res.*, **84**, 99–103 (1993).
48) Sakagami H, Jiang Y, Kusama K, Atsumi T, Ueha T, Toguchi M, Iwakura I, Satoh K, Ito H, Hatano T, Yoshida T. Cytotoxic activity of hydrolyzable tannins against human oral tumor cell lines—a possible mechanism. *Phytomedicine*, **7**, 39–47 (2000).
49) Pei X, Xiao J, Wei G, Zhang Y, Lin F, Xiong Z, Lu L, Wang X, Pang G, Jiang Y, Jiang L. Oenothein B inhibits human non-small cell lung cancer A549cell proliferation by ROS-mediated PI3K/Akt/NF-kappaB signaling pathway. *Chem. Biol. Interact.*, **298**, 112–120 (2019).
50) Tamura S, Yang GM, Koitabashi T, Matsuura Y, Komoda Y, Kawano T, Murakami N. Oenothein B, dimeric hydrolysable tannin inhibiting HCV invasion from *Oenothera erythrosepala*. *J. Nat. Med.*, **73**, 67–75 (2019).
51) Kumar A, Abbas W, Colin L, *et al.* Tuning of AKT-pathway by Nef and its blockade by protease inhibitors results in limited recovery in latently HIV infected T-cell line. *Sci Rep*, **6**, 24090 (2016).
52) Malim MH, Emerman M. HIV-1 accessory proteins—ensuring viral survival in a hostile environment. *Cell Host Microbe*, **3**, 388–398 (2008).
53) Ortega JT, Suarez AI, Serrano ML, Baptista J, Pujol FH, Rangel HR. The role of the glycosyl moiety of myricetin derivatives in anti-HIV-1 activity *in vitro*. *AIDS Res. Ther.*, **14**, 57 (2017).
54) Ono K, Nakane H, Fukushima M, Chermann JC, Barre-Sinoussi F. Differential inhibitory effects of various flavonoids on the activities of reverse transcriptase and cellular DNA and RNA polymerases. *Eur. J. Biochem.*, **190**, 469–476 (1990).
55) Pasetto S, Pardi V, Murata RM. Anti-HIV-1 activity of flavonoid myricetin on HIV-1 infection in a dual-chamber *in vitro* model. *PLOS ONE*, **9**, e115323 (2014).
56) Yin ZH, Yan HL, Pan Y, Zhang DW, Yan X. Evaluation of a flavonoid library for inhibition of interaction of HIV-1 integrase with human LEDGF/p75 towards a structure–activity relationship. *Ann. Med.*, **54**, 1590–1600 (2022).
57) Lin CH, Chang CY, Lee KR, Lin HJ, Chen TH, Wan L. Flavones inhibit breast cancer proliferation through the Akt/FOXO3a signaling pathway. *BMC Cancer*, **15**, 958 (2015).
58) Rama Reddy NR, Mehta RH, Soni PH, Makasana J, Gajbhiye NA, Ponnuchamy M, Kumar J. Next generation sequencing and transcriptome analysis predicts biosynthetic pathway of sennosides from senna (*Cassia angustifolia* Vahl.), a non-model plant with potent laxative properties. *PLOS ONE*, **10**, e0129422 (2015).
59) Esposito F, Carli I, Del Vecchio C, Xu L, Corona A, Grandi N, Piano D, Maccioni E, Distinto S, Parolin C, Tramontano E. Sennoside A, derived from the traditional Chinese medicine plant *Rheum L.*, is a new dual HIV-1 inhibitor effective on HIV-1 replication. *Phytomedicine*, **23**, 1383–1391 (2016).
60) Reicin AS, Ohagen A, Yin L, Hoglund S, Goff SP. The role of Gag in human immunodeficiency virus type 1 virion morphogenesis and early steps of the viral life cycle. *J. Virol.*, **70**, 8645–8652 (1996).
61) Dorfman T, Bukovsky A, Ohagen A, Hoglund S, Gottlinger HG. Functional domains of the capsid protein of human immunodeficiency virus type 1. *J. Virol.*, **68**, 8180–8187 (1994).
62) Wang CT, Barklis E. Assembly, processing, and infectivity of human immunodeficiency virus type 1 gag mutants. *J. Virol.*, **67**, 4264–4273 (1993).
63) Furuta RA, Shimano R, Ogasawara T, Inubushi R, Amano K, Akari H, Hatanaka M, Kawamura M, Adachi A. HIV-1 capsid mutants inhibit the replication of wild-type virus at both early and late infection phases. *FEBS Lett.*, **415**, 231–234 (1997).
64) von Schwedler UK, Stemmler TL, Klishko VY, Li S, Albertine KH, Davis DR, Sundquist WI. Proteolytic refolding of the HIV-1 capsid protein amino-terminus facilitates viral core assembly. *EMBO J.*, **17**, 1555–1568 (1998).
65) Tang S, Murakami T, Agresta BE, Campbell S, Freed EO, Levin JG. Human immunodeficiency virus type 1 N-terminal capsid mutants that exhibit aberrant core morphology and are blocked in initiation of reverse transcription in infected cells. *J. Virol.*, **75**, 9357–9366 (2001).
66) Margot NA, Gibbs CS, Miller MD. Phenotypic susceptibility to bevirimat in isolates from HIV-1-infected patients without prior exposure to bevirimat. *Antimicrob. Agents Chemother.*, **54**, 2345–2353 (2010).
67) Fujioka T, Kashiwada Y, Kilkuskie RE, Cosentino LM, Ballas LM, Jiang JB, Janzen WP, Chen IS, Lee KH. Anti-AIDS agents, 11. Betulinic acid and platanic acid as anti-HIV principles from Syzigium claviflorum, and the anti-HIV activity of structurally related triterpenoids. *J. Nat. Prod.*, **57**, 243–247 (1994).